biosensors

MDPI

Review

Progress and Prospects of Electrochemiluminescence Biosensors Based on Porous Nanomaterials

Chenchen Li [1,2], Jinghui Yang [2], Rui Xu [2], Huan Wang [1,*], Yong Zhang [2,*] and Qin Wei [1]

[1] Collaborative Innovation Center for Green Chemical Manufacturing and Accurate Detection, Key Laboratory of Interfacial Reaction & Sensing Analysis in Universities of Shandong, School of Chemistry and Chemical Engineering, University of Jinan, Jinan 250022, China; lichenchen1107@126.com (C.L.); sdjndxwq@163.com (Q.W.)

[2] Provincial Key Laboratory of Rural Energy Engineering in Yunnan, Yunnan Normal University, Kunming 650500, China; ynnu_yangjh2002@126.com (J.Y.); ecowatch_xr@163.com (R.X.)

* Correspondence: wanghuan8711@163.com (H.W.); yongzhang7805@126.com (Y.Z.)

Abstract: Porous nanomaterials have attracted much attention in the field of electrochemiluminescence (ECL) analysis research because of their large specific surface area, high porosity, possession of multiple functional groups, and ease of modification. Porous nanomaterials can not only serve as good carriers for loading ECL luminophores to prepare nanomaterials with excellent luminescence properties, but they also have a good electrical conductivity to facilitate charge transfer and substance exchange between electrode surfaces and solutions. In particular, some porous nanomaterials with special functional groups or centered on metals even possess excellent catalytic properties that can enhance the ECL response of the system. ECL composites prepared based on porous nanomaterials have a wide range of applications in the field of ECL biosensors due to their extraordinary ECL response. In this paper, we reviewed recent research advances in various porous nanomaterials commonly used to fabricate ECL biosensors, such as ordered mesoporous silica (OMS), metal–organic frameworks (MOFs), covalent organic frameworks (COFs) and metal–polydopamine frameworks (MPFs). Their applications in the detection of heavy metal ions, small molecules, proteins and nucleic acids are also summarized. The challenges and prospects of constructing ECL biosensors based on porous nanomaterials are further discussed. We hope that this review will provide the reader with a comprehensive understanding of the development of porous nanomaterial-based ECL systems in analytical biosensors and materials science.

Keywords: porous nanomaterials; electrochemiluminescence; metal-organic frameworks; covalent organic frameworks; metal-polydopamine frameworks; biosensors

Citation: Li, C.; Yang, J.; Xu, R.; Wang, H.; Zhang, Y.; Wei, Q. Progress and Prospects of Electrochemiluminescence Biosensors Based on Porous Nanomaterials. *Biosensors* **2022**, *12*, 508. https://doi.org/10.3390/bios12070508

Received: 14 June 2022
Accepted: 7 July 2022
Published: 11 July 2022

1. Introduction

Among various electroanalysis techniques, the electrochemiluminescence (ECL) method has attracted widespread attention due to its merits of high sensitivity and excellent analytical performance [1–3]. In the mid-1960s, Hercules, Santhanam, and Bard reported the first study on ECL [4,5]. Since then, the ECL technology has received wide attention from the scientific community. The ECL is a kind of new assay that combines two analytical methods: chemiluminescence (CL) and electrochemical techniques. Different from the traditional CL assay, ECL does not require an external excitation light source, so it has the advantages of a wider linear detection range, a better repeatability and anti-interference, a small background value, a good accuracy, and a high sensitivity [6,7]. The equipment and instruments for fabricating an ECL platform are usually small, and the preparation process is relatively simple and controllable [8,9]. Furthermore, ECL analysis can achieve continuous measurement, which is very popular and appropriate in the field of biochemical analysis, immunoassay, and pharmaceutical analysis. Attributing to these unique advan-

tages, it has become one of the most highly interesting research areas for researchers in the field of analytical chemistry and been regarded as a very promising analytical assay [10–12].

With the inherent merits of a large specific surface area, a high porosity, an adjustable pore size and structure, and easy modification, porous nanomaterials have great potential in the fields of multiphase catalysis, gas adsorption and separation, drug transport, and biosensing [13–16]. In the field of ECL research, it is interesting that porous nanomaterials can not only be used as carriers for loaded luminophores, catalysts for accelerating the decomposition of catalytic co-reactants, and nanoreactors for accommodating ECL systems, but also accelerate the process of substance transport and charge transfer, all of which make ECL systems based on porous nanomaterials have a strong ECL response and a high sensitivity [17–21].

Sensitivity, stability, and reproducibility are important indicators for ECL biosensors. In order to improve the performance of ECL biosensors, it is particularly important to find and develop luminophores with strong ECL signals and a high stability. Conventional luminophores, such as g-C_3N_4, have an excellent ECL response, but their sheet-like structure makes their specific surface area relatively small, which reduces the probability of contact between the luminophore and the co-reactant and seriously affects their ECL luminescence efficiency. Luminol, tris-2-2′-bipyridyl ruthenium (i.e., $Ru(bpy)_3^{2+}$), and their derivatives possess good water solubility, making it difficult to apply them alone as luminophores in aqueous solutions. Therefore, finding nanomaterials with a large specific surface area and a high porosity as carriers of ECL luminophores or preparing ECL materials with a large specific surface area and a high porosity is of extraordinary significance for the preparation of high-performance ECL biosensors. In recent years, porous nanomaterials, such as ordered mesoporous silica (OMS) [22], metal–organic frameworks (MOFs) [23], covalent organic frameworks (COFs) [24], and metal–polydopamine frameworks (MPFs) [25] have received extensive attention in the study of ECL biosensors because of their large specific surface area, high porosity, tunable pore size and structure, and easy modification. It has also demonstrated excellent performance in the detection of heavy metal ions, small molecules, proteins, and nucleic acids.

In this review, we present a detailed description of porous nanomaterial-based ECL biosensors, combining the basic construction process and the applied reaction mechanism to show the innovative applications of porous nanomaterials in ECL biosensors, as shown in Figure 1. We further discuss the challenges and the prospects of ECL systems based on porous nanomaterials. This review will enable readers to understand the relevant contents comprehensively and find more innovative applications.

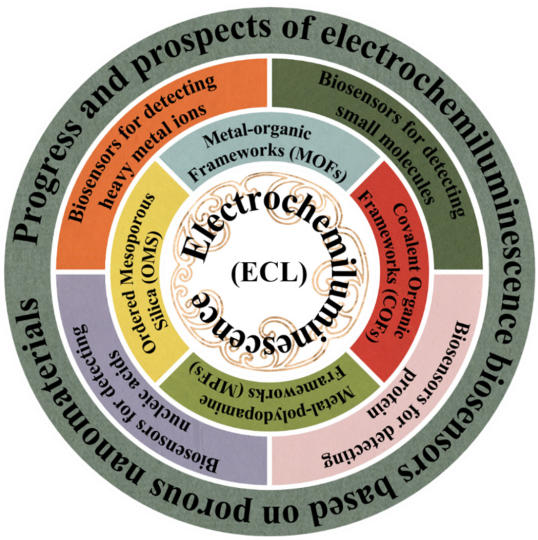

Figure 1. Schematics illustrating the application of ECL biosensors based on porous nanomaterials, as reviewed in this paper.

2. Synthesis of Porous Nanomaterials with ECL Properties

Numerous experimental results have shown that ECL biosensors based on porous nanomaterials can effectively enhance the ECL performance and enhance the accuracy of analysis [26,27]. Therefore, we firstly summarize and discuss the preparation of those porous nanomaterials with ECL properties, such as OMS, MOFs, COFs, and MPFs.

2.1. Ordered Mesoporous Silica (OMS) with ECL Properties

OMS has a wide range of applications in ECL biosensors, because of its excellent morphological characteristics, excellent stability, and simple preparation method. It is usually used as a carrier to load ECL substances by means of doping or coating techniques [28,29]. To make the discussion clearly, Table 1 summarizes several kinds of OMS-based nanocomposites being applied in the field of ECL biosensors and the corresponding synthesis strategies in recent years.

Table 1. Different synthetic strategies for OMS-based nanocomposites with ECL properties.

Nanocomposites	Methods	Luminous Body	Duration	Ref.
$mSiO_2$@CdTe@SiO_2 NSs	In situ synthesis	CdTe QDs	Microemulsion method	[30]
g-C_3N_4@ms-SiO_2	Post-synthesis modification	g-C_3N_4	Agitating	[31]
Ru-QDs@SiO_2	In situ synthesis	CN QDs, $Ru(bpy)_3^{2+}$	Microemulsion method	[32]
Ru@SiO_2	In situ synthesis	$Ru(bpy)_3^{2+}$	Self-assembly	[33]
CdTe@SiO_2	In situ synthesis	CdTe QDs	Microemulsion method	[34]
NH_2–Ru@SiO_2-NGQDs	Post-synthesis modification	CNQDs, $Ru(bpy)_3^{2+}$	Agitating	[35]
Ru@SiO_2 NPs	In situ synthesis	$Ru(bpy)_3^{2+}$	Microemulsion method	[36]
SiO_2@Ir	In situ synthesis	$Ir(ppy)_3^{2+}$	Microemulsion method	[37]
SiO_2@CQDs/AuNPs/MPBA	Post-synthesis modification	C QDs	Agitating	[38]
Ru@SiO_2	Post-synthesis modification	$Ru(bpy)_3^{2+}$	Agitating	[39]
SiO_2@Ru-NGQDs	In situ synthesis	$Ru(bpy)_3^{2+}$	Microemulsion method	[40]

As shown in Table 1, the methods for the synthesis of OMS with ECL properties are broadly divided into two categories. One is to synthesize silica nanoparticles (SiO_2 NPs) and obtain OMS-based nanocomposites through sodium hydroxide (NaOH) etching on this basis. The other is to encapsulate small organic particles in SiO_2 NPs by the microemulsion method and then obtain OMS-based nanocomposites by the high temperature calcination method [41]. The difficulty in controlling the process of etching SiO_2 NPs by NaOH makes it hard to get OMS with uniform pore channels by this etching method. Recently, the OMS prepared through the microemulsion method can effectively solve such problems [30,31]. For example, Lin et al. prepared OMS using this method, in which the luminescent g-C_3N_4 was combined with the previously prepared OMS by post-modification method as an efficient ECL probe. Based on this, the prepared sensor showed excellent correlation in the range of 0.1 nm–10 μm with an extremely low limit of detection (LOD) of 33 pM.

In another work, You et al. directly employed a microemulsion method to encapsulate $Ru(bpy)_3^{2+}$ and CN QDs in SiO_2 NPs. The electrons were transferred from CN QDs to $Ru(bpy)_3^{2+}$ through an intramolecular pathway, which shortened the distance between the electron transfer and thus improved the luminescence efficiency, yielding a self-enhanced ECL signal probe [32]. In a creative study, Jin et al. prepared a homogeneous Ru@SiO_2 NP colloidal solution and then applied it to develop Ru@SiO_2 NP nanomembranes on the surface of indium tin oxide glass (ITO) by a liquid–liquid interface self-assembly method. The obtained Ru@SiO_2 NP nanomembrane can be used as both an enhanced substrate and a luminol enricher. A self-enhanced ECL biosensor was constructed based on the intense luminescence of the Ru@SiO_2 NP nanomembrane and the enrichment of $Ru(bpy)_3^{2+}$

molecules on the surface of the Ru@SiO_2 NP nanomembrane [33]. In order to study the effect of the preparation process of nanocomposites on the properties of ECL, Shen et al. prepared CdTe@SiO_2 and SiO_2@CdTe NPs via microemulsion and post-modification methods, respectively. Interestingly, CdTe@SiO_2 with ordered mesopores is more efficient and less bio toxic for the preparation of ECL biosensors. The ECL immunosensor for the detection of methemoglobin was prepared using CdTe@SiO_2 as the signal probe with a good linearity in the range of 1.0 pg/mL to 100 ng/mL and the LOD was 0.22 pg/mL [34].

2.2. Metal–Organic Frameworks (MOFs) with ECL Properties

MOFs are a new type of porous material formed by organic ligands and metal ions or metal clusters linked by coordination bonds. Due to it inherit merits, such as a large surface area, a high porosity, abundant active sites, and a strong mass transfer capability, it has excellent performance in the field of novel materials and has a wider application in the fields of multiphase catalysis, gas adsorption and separation, drug transport, and biosensing [42–45]. Table 2 summarizes recent reported MOFs used in the field of ECL biosensors and the synthesis strategies of their composite, especially illustrating post-synthetic modifications, in situ synthesis and self-luminescent MOFs.

Table 2. Summary of different synthetic strategies for MOF composites with ECL properties.

MOF Composites	Ligands	Metal Source	Ref.
In situ synthesis			
MIL-101(Al)–NH_2	NH_2-BDC	$AlCl_3$	[46]
IRMOF-3	NH_2-BDC	$Zn(NO_3)_2$	[47]
$Ru(bpy)_3^{2+}$/NH_2-UiO-66	NH_2-BDC	$ZrCl_4$	[48]
Fe(III)-MIL-88B-NH_2	NH_2-BDC	$FeCl_3$	[49]
UiO-67	BPDC	$ZrCl_4$	[50]
GSH-Au NCS@ZIF-8	2-MI	$Zn(NO_3)_2$	[51]
Zinc Oxalate MOFs	Oxalic acid	$Zn(NO_3)_2$	[52]
Post-synthesis modifications			
Ru-MOF-5 NFs	PTA	$Zn(NO_3)_2$	[53]
Cu/Co-MOF	2-MI	$Co(NO_3)_2$, $Cu(NO_3)_2$	[54]
HH-Ru-UiO66-NH_2	NH_2-BDC	$ZrCl_4$	[55]
Co-Ni/MOF	2-MI	$Co(NO_3)_2$, Ni $(NO_3)_2$	[56]
AgNPs@Ru-MOF	NH_2-BDC	$ZrCl_4$	[57]
g-C_3N_4@NH_2-MIL-101	NH_2-BDC	$FeCl_3 \cdot 6H_2O$	[58]
Zn-Bp-MOFs	H3BTC,4,4-dipyridyl	$Zn(NO_3)_2$	[59]
Ru-PCN-777	H_3TATB	$ZrOCl_2$	[60]
Self-luminous MOFs			
Eu-MOFs	5-bop	$EuCl_3$	[61]
RuMOF NS	$[Ru(H_2dcbpy)_3]Cl_2$	$Zn(NO_3)_2$	[62]
Eu-MOF	$[Ru(H_2dcbpy)_3]Cl_2$	$Eu(NO_3)_3$	[63]
Zr-TCBPE-MOF	H_4TCBPE	$ZrCl_4$	[64]
Hf-TCBPE	H_4TCBPE	$HfCl_4$	[65]
Zr_{12}-adb	H_2adb	$ZrCl_4$	[66]
Tb-Cu-PA MOF	IPA	$TbCl_3$, $Cu(NO_3)_2$	[67]
Zn-PTC	PTC	$Zn(CH_3COO)_2$	[68]
Ru@Zr_{12}-BPDC	BPDC, H_2dcbpy	$ZrCl_4$	[69]
Cu:Tb-MOF	IPA	$TbCl_3$, $Cu(NO_3)_2$	[70]
UMV-Ce-MOF	H_3BTC	$Ce(NO_3)_3$	[71]
PTP/Eu MOF	H_3BTC	$Eu(NO_3)_3$	[72]
Ce-TCPP-LMOF	TCPP	$Ce(NO_3)_3$	[73]
Zn-MOF	Hcptpy	$ZnSO_4$	[74]

2.2.1. In Situ Synthesis

Although MOFs have a high porosity and a tunable pore size, the pore size could be fixed along with the successful preparation of MOFs. Most classical MOFs contain only micropores, which leads to the inability of guest luminophores to easily enter the MOF

interior through the pores, making the luminophore loading capacity of MOF materials greatly be reduced [75]. To solve this problem, Yang et al. wrapped the luminescence inside the MOF material by an in situ synthesis method during the MOF growth process, which resulted in a greatly enhanced loading capacity of the guest luminescence, and thus prepared the nanocomposite with a high-intensity ECL response [47].

As we all know, as an excellent luminescent substance, $Ru(bpy)_3^{2+}$ is often used in the process of constructing various ECL biosensors. For instance, Cao et al. encapsulated $Ru(Bpy)_3^{2+}$ molecules into NH_2-UiO-66 through the ligand effect during the growth of NH_2-UiO-66. The open channels or active cavities of MOFs could not only maintain the excellent ECL response of $Ru(bpy)_3^{2+}$, but also enrich the co-reactants, enabling the ECL biosensor to exhibit a highly selective and efficient ECL response, thus facilitating the ECL biosensor for ultra-sensitive and accurate analyses of the β-amyloid [48]. As shown in Figure 2D, Wang et al. applied mesoporous, hollow MIL-101(Al)-NH_2 in an ECL system by the in situ growth process and achieved a large and stable loading of $Ru(bpy)_3^{2+}$. Additionally, the authors also made poly(ethylenediamine) as a co-reactant and combined it with MIL-101(Al)-NH_2 through covalent bonding, which not only prevented the leakage of $Ru(bpy)_3^{2+}$, but also made the Ru complex produce strong and stable ECL signals through self-enhancement effect [46].

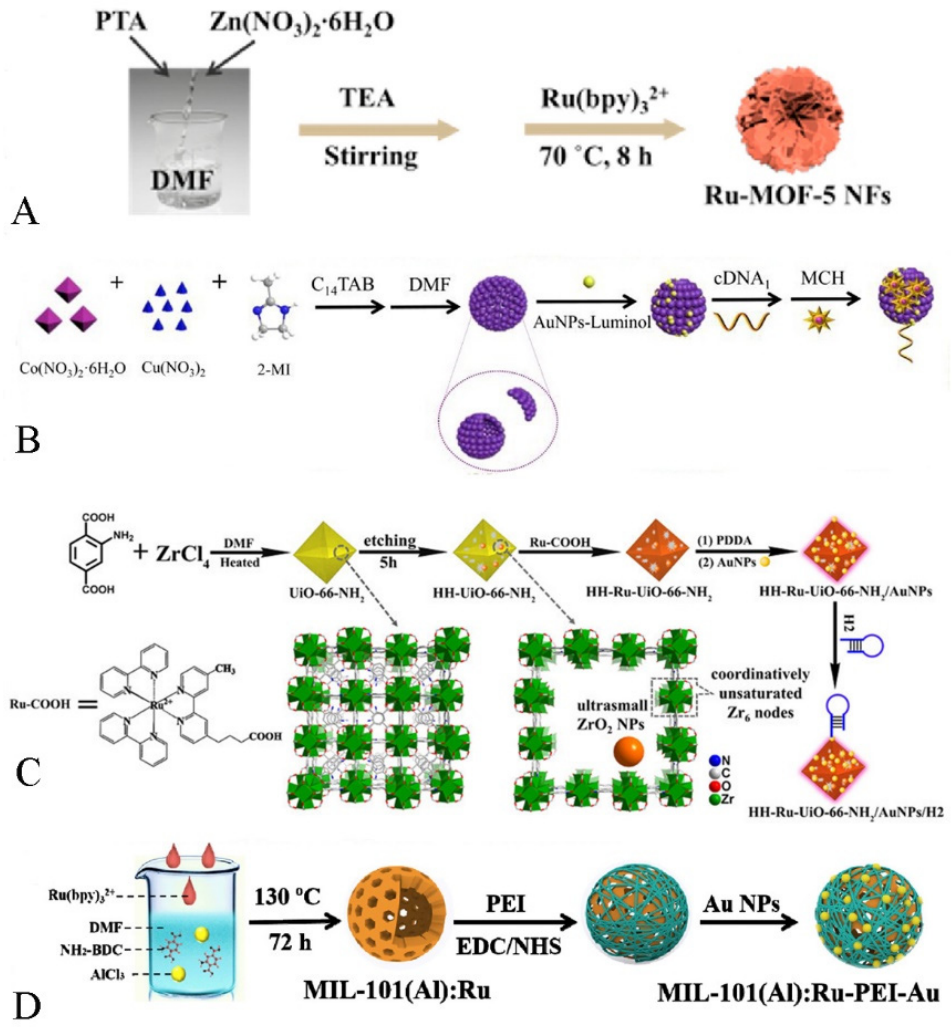

Figure 2. (**A**) The preparation of Ru-MOF-5 NFs [53]. Copyright © 2021, Elsevier. (**B**) The synthesis process of Cu/Co-MOF-luminol-AuNPs [54]. Copyright © 2021, Elsevier. (**C**) Preparation of HH-Ru-UiO-66-NH_2/Au NPs/H_2 [55]. Copyright © 2021, American Chemical Society. (**D**) The synthesis steps of MIL-101(Al): RuPEI-Au [46]. Copyright © 2019, Elsevier.

In addition to $Ru(bpy)_3^{2+}$, quantum dots (QDs) are often used in the field of ECL biosensors as an efficient and stable luminescent [76,77]. In the recent study, Tan et al. attached a large number of CdS QDs to chain-like polyethylenimine (PEI) via amide bonding, wrapped the modified PEI on the surface of MIL-53(Al), achieved massive loading of CdS QDs, and finally prepared MOF-based ECL signaling probes [78]. In another study, Deng et al. successfully encapsulated ZnSe QDs in Fe (III)-MIL-88B-NH_2 through the in situ growth process. Fe(III)-MIL-88B-NH_2 can not only achieve massive loading of ZnSe QDs, but it also contains amino groups for catalyzing the conversion of the co-reactant $S_2O_8^{2-}$ into sulfate anions ($SO_4^{\bullet -}$), which shortens the electron transfer distance and reduces the energy loss, enabling the ECL property of ZnSe QDs [49]. Although all of the above works demonstrate that the preparation of nanomaterials with ECL properties by the in situ growth method is an excellent strategy, the leakage of luminescent material is still an inevitable issue in the practical operations.

2.2.2. Post-Synthesis Modification

Post-synthesis modification is an effective means to prepare MOFs with ECL properties. The mechanism is mainly to attach luminophores to the surface of MOFs by ligand reaction, electrostatic force adsorption, or amide bonding, so that the MOFs materials, originally without ECL properties, become nanocomposites with ECL properties [79,80].

For example, As shown in Figure 2A, Wei et al. indicated that a flower-like nanomaterial with ECL properties was successfully prepared by loading $Ru(bpy)_3^{2+}$ onto the surface of MOF-5 NFs via electrostatic force adsorption, exhibiting an excellent ECL response [53].

It is worth noting that MOFs with catalytic properties act as carriers, not only to enrich the co-reactants but also to catalyze the co-reactants so that the ECL response is enhanced. As shown in Figure 2B, Zhou et al. successfully prepared nanocomposites with ECL properties by ligand bonding luminol to the MOF. The obtained hollow Cu/Co-MOF not only acted as a carrier but also could catalyze the generation of more O^{2-} from H_2O_2, which greatly enhanced the ECL response by means of this material [54].

As shown in Figure 2C, Yuan et al. connected the luminescent material $(Ru(Bpy)_2(Mcpbpy)^{2+})$ with the carrier MOF (HH-UiO-66-NH_2) through amide bonding. On the one hand, the hierarchical pore shell and hollow cavity of HH-UiO-66-NH_2 exposed more amino groups, which made the loading of the luminescent greatly increased. On the other hand, the HH-UiO-66-NH_2 surface amino group could catalyze the generation of $SO_4^{\bullet -}$ from $S_2O_8^{2-}$, which greatly shortened the distance between the co-reactant and the luminophore, making the charge transfer more efficient and thus enhancing the ECL signals [55].

2.2.3. Self-Luminous MOFs

Luminous metal-organic frameworks (LMOFs) that consist of organic bridging ligands and metal-linked nodes are novel porous nanomaterials commonly used in ECL biosensors in recent years [81]. Since LMOFs have multiple structural units, the ECL response may come from metal centers and ligands within the MOF, and the optical properties can be modulated by the interactions between the building components. Based on this, the problems of low loading of modified luminescent substances and leakage from the in situ-grown luminescent substances after MOF synthesis might be effectively solved [62,82].

Lanthanide rare-earth metal ions are an important emerging LMOFs precursor because of their unique $[Xe]4f^n$ (n = 0–14) ground-state electronic grouping pattern, which is prone to 4f–4f transitions and possesses abundant ladder electron energy levels and sharp emission bands. As shown in Figure 3, Wei et al. prepared self-luminous (Ln) metal-organic frameworks (Ln-MOFs) by hydrothermal treatment using Eu (III) ions and 5-boryl-isophthalic acid (5-bop) as precursors. The 5-bop in the triplet excited state can transfer its own energy to the Eu(III) ion by emitting ultraviolet light. When the Eu(III) ion gains energy from the ligand, it can jump to a higher energy level and release more light energy when it falls back to the ground state. The more intense ECL signal is obtained through the

antenna effect of Eu(III) ions. The prepared sensor showed a good linearity in the range of 0.005 to 100 ng/mL, and the obtained LOD was only 0.126 pg/mL [61].

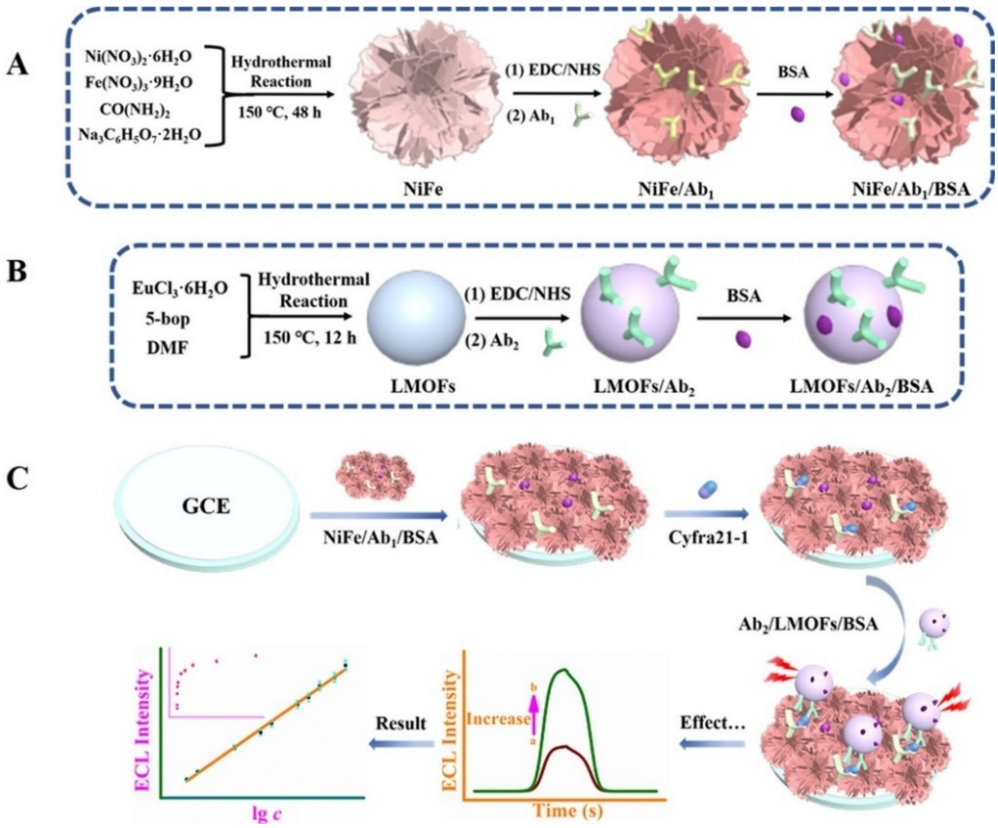

Figure 3. Preparation of NiFe Complex/Ab_1/BSA Bioconjugate (**A**), Ab_2/LMOFs/BSA Bioconjugate (**B**), and Formation Route of the Suggested Signal-Enhanced ECL Model (**C**) [61]. Copyright © 2021, American Chemical Society.

$Ru(bpy)_3^{2+}$ and its derivatives can not only prepare porous nanomaterials with ECL properties by post-synthesis modification or in situ growth, but also act as ligands for the direct synthesis of self-luminous MOFs involved in the construction of ECL biosensors [73,83].

In a pioneering work conducted by Yan et al., self-luminous Ru-MOF has been synthesized by using the autoloading $Ru(dcbpy)_3^{2+}$ and zinc ions as precursors. The obtained Ru-MOF nanosheets expose more active centers, promote closer contact with the target molecule, and have shorter diffusion distances for ions, electrons, and co-reactants. The excellent property makes the self-luminous Ru-MOF show great potential as a new Faraday cage for developing a biosensing platform [62].

As shown in Figure 4, in another interesting work, Zhao et al. synthesized a new type of Eu-MOF by a hydrothermal method using Eu (III) ions and $Ru(dcbpy)_3^{2+}$ as precursors. The Eu-MOF can undergo redox reactions and energy transfer between its ligand molecules and achieve annihilation luminescence without any additional co-reactants. At the same time, the antenna effect of Eu (III) ions in Eu-MOF is generated. In other words, when Eu (III) ions absorb the energy from the ligand, the luminescence efficiency is greatly increased, and the secondary near-infrared (NIR-II) luminescence is obtained. The prepared ECL sensor using $Eu_2[Ru(Dcbpy)_3]_3$ as the ECL signal probe was extremely resistant to interference and achieved the rapid and sensitive detection of trenbolone in the range of 5 fg/Ml–100 ng/Ml with a lower LOD of 4.83 fg/Ml [63].

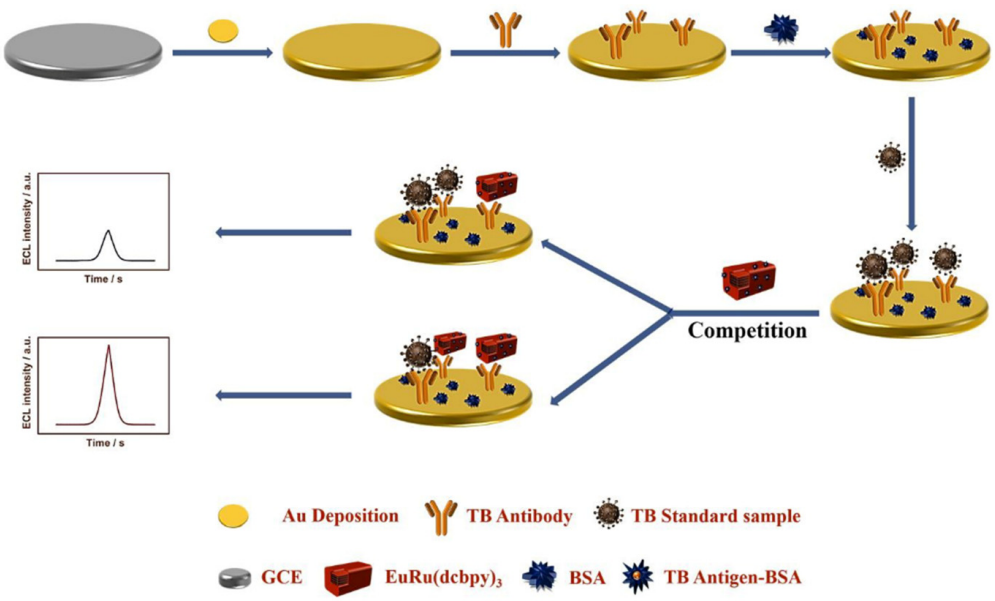

Figure 4. Annihilation luminescent Eu-MOF as a near-infrared electrochemiluminescence probe for trace detection of trenbolone [63]. Copyright © 2022, Elsevier.

Although $Ru(bpy)_3^{2+}$ and its derivatives have very common applications in the field of ECL, their high price and the biotoxicity carried by the co-reactants limit the current application of Ru-containing MOFs.

In particular, aggregation-induced ECL (AI-ECL) was firstly discovered by Luisa De Cola's team in 2017 [84]. With the continuous development in recent years, some excellent AI-ECL materials have emerged. Recently, researchers found that tetraphenylethylene (TPE) and its derivatives have the characteristics of a high ECL efficiency via easy modification. Compared with its aggregates and monomers, MOFs prepared based on TPE showed a stronger ECL response. For instance, Yuan et al. successfully prepared a novel 2D ultrathin MOF material based on the aggregation-induced emission (AIE) ligand H4ETTC and used it to construct a novel ECL biosensor for the ultrasensitive detection of CEA. The newly synthesized AIE luminogen (AIEgen)-based MOF (Hf-ETTC-MOF) yielded a higher ECL intensity and efficiency than H_4ETTC monomers, H_4ETTC aggregates and 3D bulk Hf-ETTC-MOF did [85]. As shown in Figure 5, Wei et al. synthesized a dumbbell-shaped metal–organic backbone with high luminescence efficiency by combining the aggregation-induced luminescent material H_4TCBPE with Zr(IV) ions. The obtained Zr-TCBPE-MOF possesses a more excellent ECL performance compared to the monomer and aggregates of H_4TCBPE. In addition, the authors combined Zr-TCBPE-MOF with polyethyleneimine (PEI) to prepare a unique self-reinforced Zr-TCBPE-PEI electroluminescent complex, which could effectively avoid the bio-toxicity of the co-reactant and exhibit a more dramatic ECL response. The prepared ECL sensor showed good correlation in the range of 0.0001–10 ng/mL and the lower LOD was 52 fg/mL, providing an effective way for the early and sensitive detection of small cell lung cancer [64].

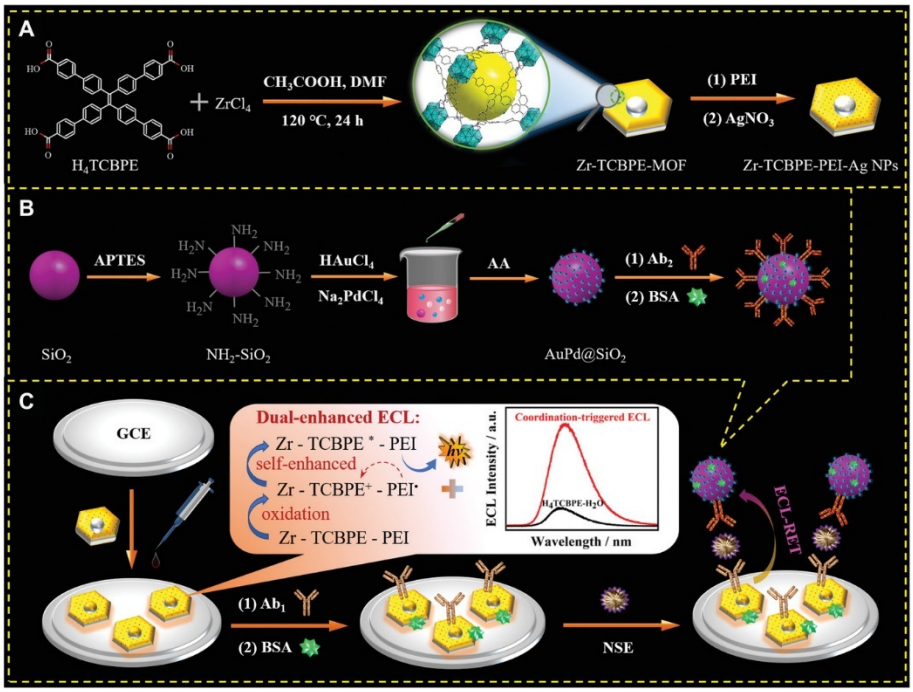

Figure 5. Schematic illustration for the synthesis of (**A**) Zr-TCBPE-PEI-Ag NPs substrate and (**B**) Ab_2-AuPd@SiO_2 bioconjugate, and (**C**) the fabrication process of the proposed ECL immunosensor with possible ECL-enhancing effects and luminescence mechanism [64]. Copyright © 2022, John Wiley and Sons.

2.3. Covalent Organic Frameworks (COFs) with ECL Properties

COFs is a class of organic porous crystalline materials composed of light elements (C, O, N, B, etc.), which are connected to each other by covalent bonds. Due to their structural designability, low density, high specific surface area, easy modification, and functionalization, COFs have been widely investigated and shown excellent prospects for applications in the fields of gas storage and separation, non-homogeneous catalysis, energy storage materials, optoelectronics, sensing, and drug delivery [86].

Although COFs materials currently synthesized by solvothermal synthesis and Knoevenagel polycondensation reaction are often used for ECL biosensors, there are not so many articles reported about the application of COFs in the development of ECL biosensors. Recently, Zhuo et al. prepared a nanocomposite with ECL properties by attaching $Ru(bpy)_3^{2+}$ to the surface of COF-LZU1. Since COF-LZU1 has a hydrophobic porous structure and TPrA is lipophilic, a large amount of TPrA in aqueous solution can be enriched into the hydrophobic inner cavity of COF-LZU1, which will shorten the distance between the luminescent material and the co-reactant and increase the concentration of co-reactant around the luminescent, resulting in a greatly enhanced ECL response [87]. However, the conductivity of COFs materials limits its application in the ECL field, which may be one of the reasons for limiting applications of COFs in the ECL biosensing study. To solve this problem, Yuan et al. provided a novel strategy. They prepared a conductive COF (HHTP-HATPCOF), as shown in Figure 6. In their work, since HHTP-HATP-COF has a large amount of ECL-emitting material and its conductive porous backbone accelerates the charge transfer in the whole backbone, the ECL response of this composite is greatly enhanced [88].

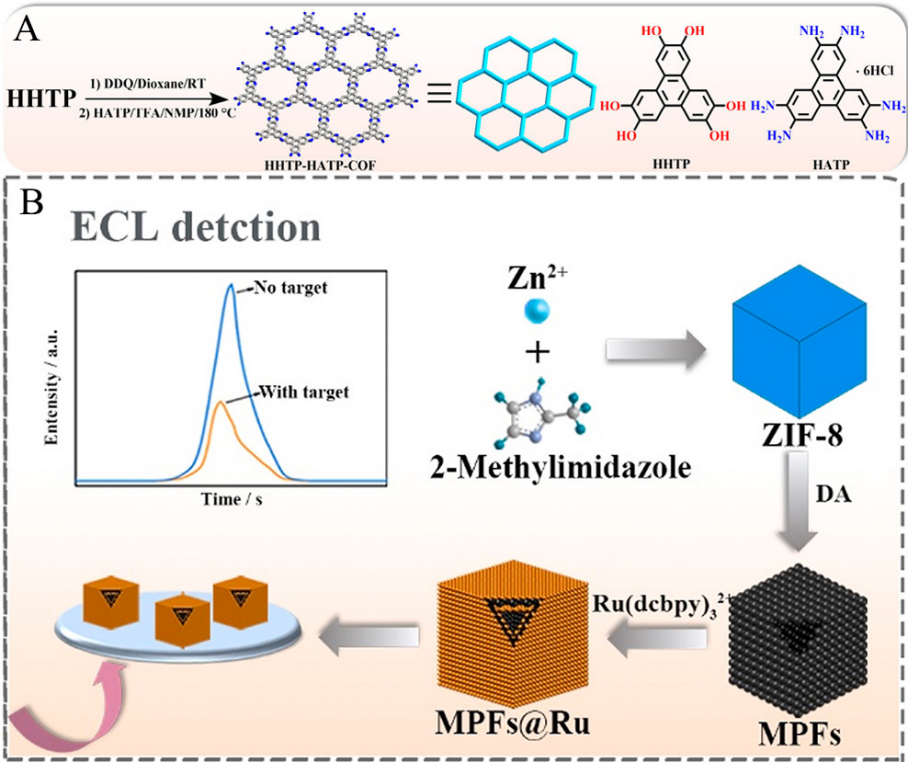

Figure 6. (**A**) Synthesis of HHTP-HATP-COF [88]. Copyright © 2022 American Chemical Society. (**B**) Preparation of MPFs@Ru [25]. Copyright © 2021 Elsevier.

2.4. Metal–Polydopamine Frameworks (MPFs) with ECL Properties

MPFs are a new hybrid material that perfectly combine the advantages of both MOFs and polydopamine (PDA) [89]. The large specific surface area and high porosity can be used to obtain a strong ECL signal by increasing the loading of luminophores. The PDA structure contains active double bonds that can chemically react with multiple groups to connect luminophores. The PDA structural fragment is a conjugated system that can generate π–π stacking with luminophores containing π bonds and thus adsorb luminophores [90,91].

As shown in Figure 6, Ma et al. prepared the MOF (ZIF-8) as the basic framework by the self-assembly method at first. After that, the hollow and porous metal–polydopamine frameworks (MPFs) were gradually formed by reacting with dopamine in a mixture of ethanol and Tris-HCl buffer, in which the polydopamine continuously replaced the original ligands through coordination reactions. Finally, the nanocomposites with ECL properties were formed by adsorption of $Ru(bpy)_3^{2+}$ through π–π stacking [25]. Although MPFs have many advantages, there are still less related studies on applying MPFs in preparing ECL biosensors. So, it is hoped that MPFs can achieve greater breakthroughs in the field of ECL biosensors through the continuous efforts of researchers.

3. Application of ECL Biosensors Based on Porous Nanomaterials

Due to their excellent stability and selectivity, porous nanomaterials have a wide range of applications in the field of ECL biosensors [92,93]. Here, we focus on introducing the applications of ECL biosensors based on porous nanomaterials in the detection of heavy metal ions, small molecules, proteins, and nucleic acids in recent years.

3.1. Biosensors for Detecting Heavy Metal Ions

It is well known that heavy metal ions have a great impact on human health and the natural environment, especially the intake of large amounts of heavy metal ions can cause irreversible damage to the human body, so the reliable and accurate detection of heavy metal ions is of great importance [94]. For example, You et al. prepared a label-free ECL biosensor

for the detection of Hg^{2+} based on the different affinity of Ru-QDs@SiO_2 nanocomposites for loading single-stranded DNA (SsDNA) and Hg^{2+}-initiated double-stranded DNA (DsDNA). When no ions of Hg^{2+} are present, single-stranded DNA is attached to the Ru-QDs@SiO_2 surface by hydrogen bonding, i.e., electrostatic force adsorption, which leads to the quenching of the ECL signal. When Hg^{2+} is present, part of the single-stranded DNA on the surface of Ru-QDs@SiO_2 is guided to form a stable dsDNA, allowing part of Ru-QDs@SiO_2 to exist in a free state, reducing the quenching of the ECL signal to single-stranded DNA [32]. Additionally, You et al. attached one end of the Hg^{2+} aptamer to NH_2-Ru@SiO_2-NGQds through an amide bond and the other end to AuNPs on the surface of the glassy carbon electrode (GCE) through an Au–S bond. When Hg^{2+} is absent, the aptamer is a long chain, and there is a large spatial site resistance between the luminescent material and the electrode surface, and, thus, the ECL response is not strong. When Hg^{2+} is present, the aptamer bends due to the formation of a thymine-Hg^{2+}-thymine (T-Hg^{2+}-T) specific structure, which draws the distance between the luminescent material and the electrode surface and reduces the spatial potential resistance, making the ECL response greatly enhanced [35].

3.2. Biosensors for Detecting Small Molecules

Table 3 summarizes ECL biosensors for detecting the small molecule based on porous nanocomposites in recent years.

Table 3. Summary of the construction of ECL biosensors based on porous nanocomposites for small molecule detection.

Analytes	Nanocomposites	Linear Range	LOD	Ref.
DES	Ru@SiO2	4.8×10^{-4}~36.0 nM	0.025 pM	[39]
DES	UiO-67	0.01 pg/mL~50 ng/mL	3.27 fg/mL	[50]
Rutin	GSH-Au NCS@ZIF-8	0.05~100 μM	10 nM	[51]
Acetamiprid	Cu/Co-MOF	0.1 μM~0.1 pM	0.018 pM	[54]
CAP	Co-Ni/MOF	1.0×10^{-13}~1.0×10^{-6} M	2.9×10^{-14} M	[56]
ATX-a	AgNPs@Ru-MOF	0.001~1 mg/mL	0.00034 mg/mL	[57]
Trenbolone	Eu-MOF	5 fg/mL~100 ng/mL	4.83 fg/mL	[63]
IMI	UMV-Ce-MOF	2–120 nM	0.34 nM	[71]
Lincomycin	PTP/Eu MOF	0.1 mg/mL~0.1 ng/mL	0.026 ng/mL	[72]

Chloramphenicol (CAP) is a broad-spectrum antibiotic that can effectively treat a variety of microbial infections such as typhoid fever, meningitis, and salmonellosis. Since the middle of last century, it has become a widely used antibiotic because of its low production cost and good drug stability. However, many studies in recent years have shown that excessive intake of CAP can inhibit bone marrow hematopoiesis, which in turn can severely damage the human hematopoietic system. Therefore, it is necessary to establish a rapid and sensitive detection method to accurately monitor CAP residues in the aqueous environment. Chen et al. synthesized black phosphorus QDs (BPQDs) into PTC-NH_2 solution to synthesize nanocomposites with ECL properties (BP/PTC-NH_2). An efficient and sensitive ECL sensor was prepared to detect CAP by combining BP/PTC-NH_2 with Co-Ni/MOF as an ECL emitter via electrostatic adsorption. The composite material of co-Ni/MOF has a good catalytic effect and can catalyze the co-reactant $K_2S_2O_8$ to generate more $SO_4^{\bullet -}$, which enhances the ECL response of the system. When CAP is present, the specific recognition of the aptamer makes the aptamer detach from the surface of the luminescent material, which reduces the burst of the aptamer for the ECL response and thus enhances the ECL signal [56].

Anatoxin-a (ATX-a) is a highly toxic alkaloid neurotoxin isolated from Anabaena flos-aquae (e.g., a semi-lethal dose of 200 μg/mL for rats) with a strong nicotine-like neuromuscular depolarization blocking effect, and animals poisoned will experience myofascicular twitching, corneal inversions, respiratory muscle spasms, and the animals will

show symptoms such as muscle bundle convulsion, corkscrew, respiratory muscle spasm, and salivation after poisoning. Therefore, it is of great interest to find a rapid and sensitive test for the detection of ATX-a in water. As shown in Figure 7, Wang et al. proposed an ECL biosensor based on the ECL-RET strategy with a low background signal by means of double burst and dual stimulus response. The prepared ECL biosensor provides an accurate signal output for the ultrasensitive detection of ATX-a. Specifically, the authors wrapped $Ru(bpy)_3^{2+}$ in UiO-66-NH_2 by the in situ growth method to act as an ECL signal probe, wrapped it with silver nanoparticle (AgNPs) shells as the main bursting agent, and tightly bound it to DNA-ferrocene (Fc). The AgNPs play an important role in the whole system, not only to close the permanent pore of UiO-66-NH_2 and prevent the leakage of $Ru(bpy)_3^{2+}$, but also to act as a quencher to quench the ECL signal of $Ru(bpy)_3^{2+}$. Not only that, the AgNPs generated in situ can specifically recognize and break the substrate chain, generating an "On" signal, which helps to avoid false positive results. Thus, an ultra-sensitive detection of ATX-a was achieved in the range of 0.001 to 1 mg/mL, and the LOD was estimated to be 0.00034 mg/mL [57].

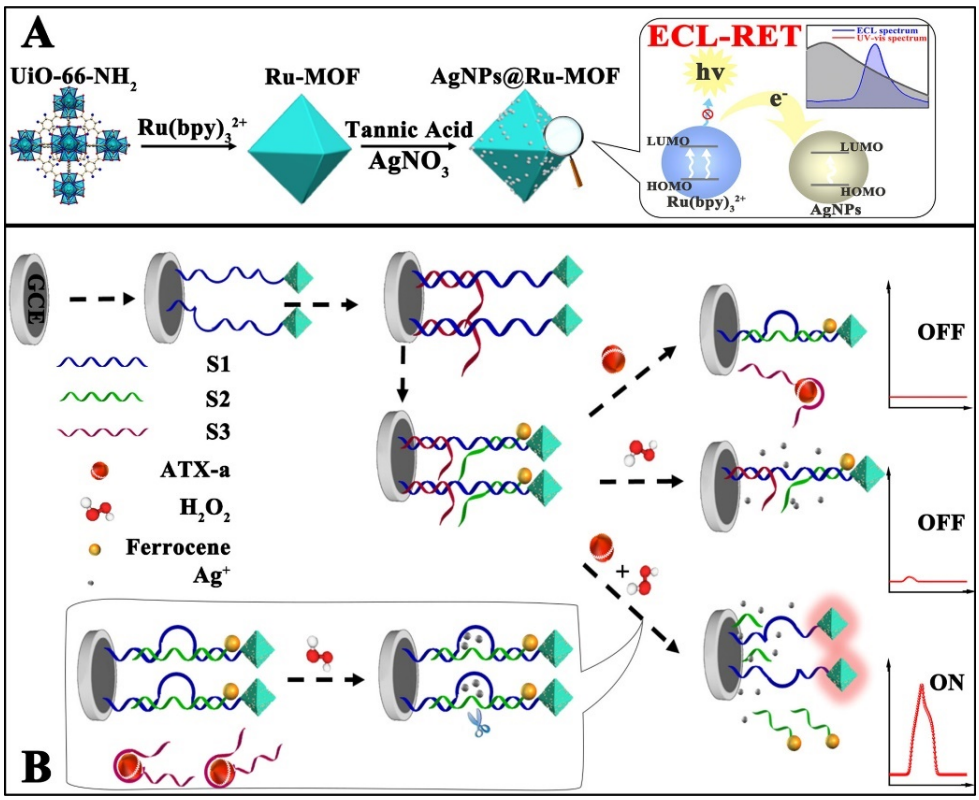

Figure 7. Schematic illustration of in situ generation of AgNPs@Ru-MOF and progress of ECL-RET (**A**), and the response process of ECL-RET aptasensor for ATX-a (**B**) [57]. Copyright © 2021, American Chemical Society.

3.3. Biosensors for Detecting Protein

Cancer has now become a global difficult-to-treat disease, and it is well known that the treatment of early-stage cancer patients saves much more labor, money, and time than that of late-stage cancer patients, so early diagnosis of cancer is of great significance. The ECL analysis method provide a potential assay for the sensitive and selective detection of certain cancer disease-related biomarkers by coupling antigen–antibody specific binding with ECL technology. As shown in Table 4, we summarize some of the porous nanomaterial-based ECL sensors used for protein detection in recent years.

Table 4. Summary of the construction of ECL biosensors based on porous nanocomposites for protein detection.

Analytes	Nanocomposites	Linear Range	LOD	Ref.
HE4	g-C_3N_4@ms-SiO_2	10^{-5} to 10 ng/mL	3.3×10^{-6} ng/mL	[31]
PSA	Ru@SiO_2	10^{-15} to 10^{-6} g/mL	0.169 fg/mL	[33]
AFP	CdTe@SiO_2	1.0 pg/mL to 100 ng/mL	0.22 pg/mL	[34]
HAase	Ru@SiO_2 NPs	2 to 60 U/mL	2 U/mL	[36]
BNPT	SiO_2@Ir	0.1 ng/mL to 200 ng/mL	0.03 ng/mL	[37]
AFP	SiO_2@CQDs/AuNPs/MPBA	0.001 to 1000 ng/m L	0.0004 ng/mL	[38]
PCT	MIL-101(Al)–NH_2	0.0005 ng/mL to 100 ng /mL	0.18 pg/mL	[46]
cTnI	IRMOF-3	1 fg/mL to 10 ng/mL	0.46 fg/mL	[47]
SCCA	Fe(III)-MIL-88B-NH_2	0.0001 to 100 ng/mL	31 fg/mL	[49]
Aβ	Zinc Oxalate MOFs	100 fg/mL to 50 ng/mL	13.8 fg/mL	[52]
NSE	Ru-MOF-5 NFs	0.0001 ng/mL to 200 ng/mL	0.041 pg/mL	[53]
Thrombin	HH-Ru-UiO66-NH_2	100 fM to 100 nM	31.6 fM	[55]
PCT	NH_2-MIL-101	0.014 pg/mL to 40 ng/mL	3.4 fg/mL	[58]
MUC1	Zn-Bp-MOFs	1 pg/mL to 10 ng/mL	0.23 pg/mL	[59]
MUC1	Ru-PCN-777	100 fg/mL to 100 ng/mL	33.3 fg/mL	[60]
CYFRA21-1	Eu-MOFs	0.005 to 100 ng/mL	0.126 pg/mL	[61]
cTnI	RuMOFNSs	1 fg/mL to 10 ng/mL	0.48 fg/mL	[62]
NSE	Zr-TCBPE-MOF	0.0001 to 10 ng/mL	52 fg/mL	[64]
MUC1	Hf-TCBPE	1 fg/mL to 1 ng/mL	0.49 fg/mL	[65]
MUC1	Zr_{12}-adb	1 fg/mL to 100 ng/mL	100 ng/mL	[66]
CYFRA21-1	Tb-Cu-PA MOF	0.01 to 100 ng/mL	2.6 pg/mL	[67]
MUC1	Ru@Zr_{12}-BPDC	1 fg/mL to 10 ng/mL	0.14 fg/mL	[69]
ProGRP	Cu:Tb-MOF	1.0 pg/mL to 50 ng/mL	0.68 pg/mL	[70]

Mucin-1 (MUC1) is an important transmembrane glycoprotein that is considered an important biomarker for colon, breast, ovarian, and lung cancers. Recently, Yuan et al. prepared a novel multivacancy nanocomposite (Hf-TCBPE) with ECL properties based on the principle of matrix coordination-induced ECL (MCI-ECL) enhancement. The MOF constructed by Hf ions and TCBPE ligands has its internal spatial structure fixed, which restricts the intramolecular free motion of TCBPE and suppresses the nonradiative relaxation, and the high porosity of Hf-TCBPE enables both internal and external excitation of TCBPE, which greatly enhances its ECL response. An ECL biosensor for the detection of mucin 1 (MUC 1) was constructed by combining HF-TCBPE with a phosphate-terminated ferrocene (FC)-labeled hairpin DNA aptamer (FC-HP3) as a signal probe (HF-TCBPE/FC-HP3) with the aid of an exonuclease III (Exo III) cyclic amplification strategy [65]. Another novel piece of research is that Xiao et al. discovered that the ECL of the material could be enhanced by restricting intramolecular motion, and based on this principle, a two-dimensional ultrathin MOF (Zr_{12}-ABD) with AI-ECL properties was prepared. In 2D MOF, the ligand 9,10-anthracene dibenzoate is immobilized, which restricts its intramolecular motion and suppresses the energy loss due to spin, allowing more energy to be released in the form of light energy and significantly enhancing the ECL response. Meanwhile, the ultrathin multivacancy structure of 2D MOF not only allows more co-reactants to enter the interior of MOF, but also reduces the migration distance between the electrons, ions, and co-reactants due to the smaller spatial site resistance, which reduces the energy loss and further enhances the ECL response of Zr_{12}-ABD. A biosensor for the sensitive detection of mucin 1 was prepared by combining Zr_{12}-ABD nanomaterials with a bipedal walking molecular machine. The ECL signal decreased with an increasing concentration of MUC1 in the range of 1 fg/mL to 100 ng/mL, showing a good linearity, and the LOD of the prepared ECL sensor was only 0.25 fg/mL [66].

CYFRA21-1 is considered to be a tumor marker mainly used for the detection of lung cancer and is especially valuable for the diagnosis of non-small cell lung cancer (NSCLC). In a study, Wei et al. creatively prepared a rare earth (Ln) metal–organic backbone (LMOF) with ECL properties. Ln-MOF was prepared from a precursor containing Eu(III) ions and

5-boronic acid isophthalic acid (5-bop). The ligand 5-bop produces a triplet state upon UV excitation, which triggers the red light emission of Eu(III) ions and enhances the ECL response. The electron-deficient boric acid reduces the energy transfer efficiency from the triplet state of 5-bop to the Eu(III) ion, resulting in both being efficiently excited under a single excitation. In addition, the synthesized flower-like Ni/Fe composites (Ni/Fe 1:1) have more active centers, higher stability, and good electrical conductivity by gradually adjusting the atomic ratio of Ni/Fe. An ECL immunosensor for the highly sensitive detection of CYFRA21-1 was prepared using Ln-MOF as the ECL emitter and flower-like Ni/Fe composite as the substrate, and the prepared Eu-LMOF showed good performance characteristics in the ECL immunoassay with the LOD of 0.126 pg/mL [61].

Ju et al. synthesized a MOF with ECL properties (Tb-Cu-PA MOF) using luminescent Tb^{3+} and catalytic Cu^{2+} ions as metal linkers and isophthalic acid (PA) as a bridging ligand. The doping of Cu^{2+} significantly reduced the size of the MOF and produced a strong and stable ECL signal. Therefore, the authors prepared a novel ECL immunosensor for the sensitive detection of CYFRA21-1 by using the synthesized Tb-Cu-PA MOF as an ECL emitter and Ni–Co layered double hydroxide (LDH) containing ZIF-67 nanocubes as a substrate. Compared with ZIF-67, ZIF-67@LDH has larger specific surface area and more active centers. After depositing palladium nanoparticles (Pt NPs) on ZIF-67@LDH nanocubes, it can improve the charge transport and electrocatalytic performance, catalyze $S_2O_8{}^{2-}$ to produce more $SO4^{\bullet-}$, and obtain more intense ECL signals. The linear range of the successfully prepared ECL immunosensor was 0.01–100 ng/mL with a LOD of 2.6 pg/mL [67].

Except for the biomarkers, biological enzymes also play an irreplaceable role in human life activities. The abnormal activity of certain enzymes can lead to disorders in human functions. Therefore, to develop a rapid and highly sensitive measurement of some enzymes is important for clinical diagnosis and basic biochemical research. The sensitive detection of thrombin (TB), an important biomarker that plays an important role in hemostasis and thrombosis, has attracted great interest. In a study, Yuan et al. prepared a hollow graded MOF (HH-UiO-66-NH_2) with graded pore shells by a simple hydrothermal etching method and used it as a carrier to load $Ru(bpy)_2(Mcpbpy)^{2+}$, and successfully prepared a nanocomposite (HH-Ru-UiO66-NH_2) with an excellent ECL signal. The multilayer structure and cavity of HH-UIO-66-NH_2 allowed the macromolecule $Ru(bpy)_2(Mcpbpy)^{2+}$ to be immobilized not only on the surface of MOF but also on the interior of MOF, which led to a significant increase in the loading of MOF on the luminescent group. On the other hand, the multilayer structure of HH-UIO-66-NH_2 allowed the rapid diffusion of reactants, ions, and electrons, thus promoting the excitation of more luminophores. In addition, the etched HH-UIO-66-NH_2 exposes more amino groups, which can catalyze the co-reactant $K_2S_2O_8$ to generate $SO_4{}^{\bullet-}$ radicals, and thus greatly improve the ECL luminophore utilization rate. Ultimately, the authors used HH-RU-UIO-66-NH_2 as a high-performance ECL probe combined with a catalytic hairpin assembly (CHA) enzyme-free amplification technology to construct an ECL biosensor for the ultrasensitive detection of TB. The successfully prepared ECL immunosensor exhibited a good linearity in the range of 100 fM–100 nM, and the LOD of the prepared ECL sensor was only 31.6 fM [55].

Hyaluronidase (Haase) is another general term for enzymes that oligomerize hyaluronic acid (HA). It can decrease the activity of hyaluronic acid in the body, thereby increasing the ability of fluid permeation in tissues. In recent years, Haase has been considered as a potential tumor marker. In a recent work, Lin et al. designed a slow-release system based on a hydrogel constructed of HA with polyethyleneimine (PEI) and a large amount of $Ru(bpy)_3{}^{2+}$-doped silica nanoparticles (Ru@SiO_2NPs) stably dispersed in the hydrogel as an ECL signaling probe. When Haase is present, the hydrogel is decomposed by Haase, allowing Ru@SiO_2NPs to escape from the hydrogel into the supernatant, and the concentration of Haase can be quantified by the ECL signal generated from the supernatant. Compared with previous work, this biosensor does not require large amounts of HA to

immobilize the signal probe or tedious centrifugation methods to reduce background interference, and thus has an excellent sensitivity and selectivity [36].

3.4. Biosensors for Detecting Nucleic Acids

MicroRNAs are small single-stranded non-coding RNAs of about 19–23 nucleotides. Although the first microRNAs were discovered as early as 1993, only in recent years has the diversity and breadth of this class of genes been revealed. It is hypothesized that vertebrate genomes have up to 1000 different miRNAs, regulating at least 30% of gene expression. Moreover, microRNAs are also considered to be reliable biomarkers for various cancers and genetic diseases. With the continuous development of biotechnology, scientists have combined DNA amplification strategies, such as target cyclic amplification (TRC), catalytic hairpin assembly (CHA), and strand displacement amplification (SDA). With the ECL technique to prepare a number of efficient and sensitive ECL biosensors for the detection of nucleic acids [95,96]. As shown in Table 5, an increasing number of ECL biosensors based on porous nanocomposites have been successfully developed and applied for the sensitive detection of nucleic acids in recent years.

Table 5. Summary of the construction of ECL biosensors based on porous nanocomposites for nucleic acids detection.

Analytes	Nanocomposites	Linear Range	LOD	Ref.
miRNA-182	$mSiO_2$@CdTe@SiO_2 NSs	0.1 to 100 pM	33 fM	[30]
microRNA-21	Zn-PTC	100 aM to 100 pM	29.5 aM	[68]
miRNA-133a	Zn-MOF	50 aM to 50 fM	35.8 aM	[74]
microRNA-21	Py-sp2c-COF	100 aM to 1 nM	46 aM	[97]
microRNA-21	Co-MOF-ABEI/$Ti_3C_2T_x$	0.00001 to 10 nM	3.7 fM	[98]
miRNA-155	RuMOFs	0.8 fM to 1.0 nM	0.3 fM	[99]

Recently, Yuan et al. found that when polycyclic aromatic hydrocarbons (PAHs) were used as ligands for the synthesis of MOFs, the aggregation-induced burst (ACQ) effect of PAHs could be effectively eliminated by coordination immobilization of the ligands as a way to improve the strength and efficiency of ECL. Based on this principle, a MOF (Zn-PTC) with AI-ECL properties was prepared. The molecular spacing of PTC was effectively increased by ligand immobilization in the MOF, thus eliminating the ACQ effect and resulting in a greatly enhanced ECL response of Zn-PTC. In addition, the PTCs in Zn-PTC stacked in an edge-to-edge manner to form J-type aggregates, which also promoted the enhanced ECL response. Based on the good ECL performance, an ECL biosensor for the sensitive detection of microRNA-21 was constructed by using Zn-PTC as an ECL signaling probe in combination with a dual amplification strategy of a nucleic acid exonuclease III-stimulated targeting cycle and DNAzyme-assisted cycling. The ECL sensor was able to detect microRNA-21 in the range of 100 aM to 100 pM with an efficient and sensitive LOD of 29.5 aM [68].

Additionally, Yuan's team prepared a Py-sp2 carbon-conjugated nanosheet (Py-sp2c-CON) with ECL properties based on the condensation reaction of tetrakis(4-formylphenyl)pyrene (TFPPy) and 2,2′-(1,4-phenylene)diacetonitrile. The porous ultra-thin structure of Py-sp2c-CON can effectively shorten the material transport distance and energy transfer process of electrons, ions, and co-reactants ($S_2O_8^{2-}$), which greatly enhances the ECL response of luminescent substances. Based on these advantages, an ECL biosensor for microRNA-21 detection was prepared using the Py-sp2c-CON/$S_2O_8^{2-}$/Bu_4NPF_6 system, which has a wide linear response (100 am~1 nM) and a lower LOD (46 am) [97].

In another study, a highly efficient and sensitive ECL biosensor for the detection of miRNA-21 was constructed using a Co-MOF-ABE/Ti_3C_2Tx composite as an ECL luminescent substance combined with a DSN-assisted target recovery signal amplification strategy. Co-MOF has a large specific surface area and thus can be loaded with abundant luminophores. Not only that, Co-MOF also exhibits excellent catalytic properties, and

the ECL response of the composite is greatly improved by these factors. The successfully prepared ECL immunosensor achieved sensitive detection of miRNA-21 in the range of 0.00001 and 10 nM with a LOD of only 3.7 fM [98].

4. Conclusions and Outlooks

In one word, we give a comprehensive overview of the recent progress in the construction of ECL biosensors based on porous nanomaterials. Due to their large specific surface area, high porosity, large number of active sites, adjustable structure, easy modification, and good biocompatibility, porous nanomaterials, such as OMS, MOFs, COFs, and MPFs, have a large number of applications in the field of ECL biosensors. The preparation of different types of porous nanomaterials with ECL properties were summarized and their applications in the detection of heavy metal ions, small molecules, proteins, and nucleic acids. In conjunction with the representative articles, we summarize the advantages of porous nanomaterials in the field of ECL biosensors.

Firstly, porous nanomaterials with a large specific surface area and a variety of different functional groups can provide a good modification basis for loading ECL luminescent substances, which is beneficial for the construction of high-performance ECL biosensors.

Secondly, the high porosity and adjustable pore size can provide the basis for the preparation of composites by means of various synthesis methods, such as in situ growth and encapsulation, and it can additionally provide good channels for energy transfer and substance transport such as ions, electrons, and co-reactants.

Thirdly, the loading of co-reactants and luminescent substances in an all-in-one structure or the loading of two luminescent substances with different wavelengths in the same structure based on the RET effect can shorten the substance and charge transfer paths between the luminescent substances and basis, and thus can realize the self-enhancement of the ECL response, which reflects the superiority of the synergistic effect.

Although greater progress has been made in ECL biosensors based on porous nanomaterials, there are still some problems to be paid attention to that may limit the application of porous nanomaterials in this field. One of the main issues is that most porous nanomaterials with ECL properties in the field of macromolecular sensing still suffer from a high excitation voltage and a low luminescence efficiency because of their high impedance. Therefore, the development of luminescent substances with a high conductivity, a low voltage excitation, and a high ECL efficiency are also discussed in detail. Although porous nanomaterials have been widely used in the field of ECL biosensors, the limitations of synthesis methods and synthetic materials prevent the application of organic composite materials with a poor electrical conductivity (e.g., COFs materials) from being widely used. It is worth noting that the application of MPFs and AI-ECL materials are still in the initial stage, and so is the design of COFs materials with a high electrical conductivity. Based on this stage, the design of COFs with a high conductivity and the construction of ECL biosensors based on MPFs open new directions in the field of ECL.

1. AI-ECL materials or techniques are still a new research direction in the field of sensors. The types of ligands currently used are relatively single, and the AI-ECL mechanism of most materials is almost the same. Therefore, the search for new organic ligands, the study of a new AI-ECL material reaction mechanism, and the design of synthesizing innovative structures of AI-ECL materials will be hot directions.
2. Most of the current porous nanomaterials with functional groups have poor electrical conductivities, and the functional group types are relatively single. How to prepare porous nanomaterials with a high conductivity and multiple functional groups and how to combine them with luminescent substances with different functional groups to achieve the synergistic effect between each group are still needed to pay more attention to.
3. At present, most of the ECL biosensors based on porous nanomaterials are still in the laboratory stage. The instrumentation and experimental conditions required for testing experiments are relatively strict. Consequently, combining ECL sensors with

microfluidics and smartphone detection to build portable devices and instruments for environmental detection remains a great challenge.

Author Contributions: C.L. wrote the main text of the manuscript. H.W. and Y.Z. supervise C.L. and gave guidance to write the manuscript. C.L. and J.Y. are responsible for writing the Section 2. R.X., Y.Z. and Q.W. are responsible for writing the Section 3. Y.Z. is responsible for organizing the whole review paper and language editing and wrote the Section 4. Y.Z., R.X. and H.W. provide the fundings for this work. All authors have read and agreed to the published version of the manuscript.

Funding: This work was financially supported by the National Natural Science Foundation of China (21775053), the Natural Science Foundation of Shandong Province (2019GSF111023), and the Applied Basic Research Foundation of Yunnan Province (202201AS070020, 202201AU070061).

Institutional Review Board Statement: Not applicable.

Informed Consent Statement: Not applicable.

Data Availability Statement: Not applicable.

Conflicts of Interest: The authors declare that they have no known competing financial interest or personal relationships that could have appeared to influence the work reported in this paper.

References

1. Chen, S.; Ma, H.; Padelford, J.W.; Qinchen, W.; Yu, W.; Wang, S.; Zhu, M.; Wang, G. Near Infrared Electrochemiluminescence of rod-shape 25-atom AuAg nanoclusters that is hundreds-fold stronger than that of $Ru(bpy)_3^{2+}$ standard. *J. Am. Chem. Soc.* **2019**, *141*, 9603–9609. [CrossRef] [PubMed]
2. Kim, T.; Kim, H.J.; Shin, I.-S.; Hong, J.-I. Potential-dependent electrochemiluminescence for selective molecular sensing of cyanide. *Anal. Chem.* **2020**, *92*, 6019–6025. [CrossRef] [PubMed]
3. Zhang, J.; Jin, R.; Jiang, D.; Chen, H.Y. Electrochemiluminescence-based capacitance microscopy for label-free imaging of antigens on the cellular plasma membrane. *J. Am. Chem. Soc.* **2019**, *141*, 10294–10299. [CrossRef] [PubMed]
4. Hercules David, M. Chemiluminescence resulting from electrochemically generated species. *Science* **1964**, *145*, 808–809. [CrossRef] [PubMed]
5. Santhanam, K.S.V.; Bard, A.J. Chemiluminescence of electrogenerated 9,10-diphenylanthracene anion radical1. *J. Am. Chem. Soc.* **1965**, *87*, 139–140. [CrossRef]
6. Liu, Z.; Qi, W.; Xu, G. Recent advances in electrochemiluminescence. *Chem. Soc. Rev.* **2015**, *44*, 3117–3142. [CrossRef]
7. Miao, W. Electrogenerated chemiluminescence and its biorelated applications. *Chem. Rev.* **2008**, *108*, 2506–2553. [CrossRef] [PubMed]
8. Qi, H.; Zhang, C. Electrogenerated chemiluminescence biosensing. *Anal. Chem.* **2020**, *92*, 524–534. [CrossRef]
9. Chen, Y.; Zhou, S.; Li, L.; Zhu, J.J. Nanomaterials-based sensitive electrochemiluminescence biosensing. *Nano Today* **2017**, *12*, 98–115. [CrossRef]
10. Hu, L.; Xu, G. Applications and trends in electrochemiluminescence. *Chem. Soc. Rev.* **2010**, *39*, 3275–3304. [CrossRef] [PubMed]
11. Ma, C.; Cao, Y.; Gou, X.; Zhu, J.-J. Recent progress in electrochemiluminescence sensing and imaging. *Anal. Chem.* **2020**, *92*, 431–454. [CrossRef]
12. Farka, Z.; Juřík, T.; Kovář, D.; Trnková, L.; Skládal, P. Nanoparticle-based immunochemical biosensors and assays: Recent advances and challenges. *Chem. Rev.* **2017**, *117*, 9973–10042. [CrossRef]
13. Wang, R.; Xi, S.C.; Wang, D.Y.; Dou, M.; Dong, B. Defluorinated porous carbon nanomaterials for CO_2 capture. *ACS Appl. Nano Mater.* **2021**, *4*, 10148–10154. [CrossRef]
14. Jin, L.; Lv, S.; Miao, Y.; Liu, D.; Song, F. Recent development of porous porphyrin-based nanomaterials for photocatalysis. *ChemCatChem* **2021**, *13*, 140–152. [CrossRef]
15. Han, T.; Cao, Y.; Chen, H.Y.; Zhu, J.J. Versatile porous nanomaterials for electrochemiluminescence biosensing: Recent advances and future perspective. *J. Electroanal. Chem.* **2021**, *902*, 115821. [CrossRef]
16. Xu, Y.; Wang, C.; Wu, T.; Ran, G.; Song, Q. Template-free synthesis of porous fluorescent carbon nanomaterials with gluten for intracellular imaging and drug delivery. *ACS Appl. Mater. Interfaces* **2022**, *14*, 21310–21318. [CrossRef]
17. Li, J.; Luo, M.; Yang, H.; Ma, C.; Cai, R.; Tan, W. Novel dual-signal electrochemiluminescence aptasensor involving the resonance energy transform system for kanamycin detection. *Anal. Chem.* **2022**, *94*, 6410–6416. [CrossRef]
18. Wang, S.; Zhao, Y.; Wang, M.; Li, H.; Saqib, M.; Ge, C.; Zhang, X.; Jin, Y. Enhancing luminol electrochemiluminescence by combined use of cobalt-based metal organic frameworks and silver nanoparticles and its application in ultrasensitive detection of cardiac troponin I. *Anal. Chem.* **2019**, *91*, 3048–3054. [CrossRef]
19. Han, Q.; Wang, C.; Liu, P.; Zhang, G.; Song, L.; Fu, Y. Achieving synergistically enhanced dual-mode electrochemiluminescent and electrochemical drug sensors via a multi-effect porphyrin-based metal-organic framework. *Sens. Actuators B Chem.* **2021**, *330*, 129388. [CrossRef]

20. Wang, C.; Liu, L.; Liu, X.; Chen, Y.; Wang, X.; Fan, D.; Kuang, X.; Sun, X.; Wei, Q.; Ju, H. Highly-sensitive electrochemiluminescence biosensor for NT-proBNP using MoS_2@Cu_2S as signal-enhancer and multinary nanocrystals loaded in mesoporous UiO-66-NH_2 as novel luminophore. *Sens. Actuators B Chem.* **2020**, *307*, 127619. [CrossRef]
21. Liao, B.Y.; Chang, C.J.; Wang, C.F.; Lu, C.H.; Chen, J.K. Controlled antibody orientation on Fe_3O_4 nanoparticles and CdTe quantum dots enhanced sensitivity of a sandwich-structured electrogenerated chemiluminescence immunosensor for the determination of human serum albumin. *Sens. Actuators B Chem.* **2021**, *336*, 129710. [CrossRef]
22. Wei, X.; Luo, X.; Xu, S.; Xi, F.; Zhao, T. A Flexible Electrochemiluminescence sensor equipped with vertically ordered mesoporous silica nanochannel film for sensitive detection of clindamycin. *Front. Chem.* **2022**, *10*, 2296–2646. [CrossRef] [PubMed]
23. Song, X.; Zhao, L.; Luo, C.; Ren, X.; Yang, L.; Wei, Q. Peptide-based biosensor with a luminescent copper-based metal–organic framework as an electrochemiluminescence emitter for trypsin assay. *Anal. Chem.* **2021**, *93*, 9704–9710. [CrossRef] [PubMed]
24. Li, Y.; Yang, F.; Yuan, R.; Zhong, X.; Zhuo, Y. Electrochemiluminescence covalent organic framework coupling with CRISPR/Cas12a-mediated biosensor for pesticide residue detection. *Food Chem.* **2022**, *389*, 133049. [CrossRef] [PubMed]
25. Ma, Y.; Yu, Y.; Mu, X.; Yu, C.; Zhou, Y.; Chen, J.; Zheng, S.; He, J. Enzyme-induced multicolor colorimetric and electrochemiluminescence sensor with a smartphone for visual and selective detection of Hg^{2+}. *J. Hazard. Mater.* **2021**, *415*, 125538. [CrossRef]
26. Li, X.; Yu, S.; Yan, T.; Zhang, Y.; Du, B.; Wu, D.; Wei, Q. A sensitive electrochemiluminescence immunosensor based on $Ru(bpy)_3^{2+}$ in 3D CuNi oxalate as luminophores and graphene oxide–polyethylenimine as released $Ru(bpy)_3^{2+}$ initiator. *Biosens. Bioelectron.* **2017**, *89*, 1020–1025. [CrossRef]
27. Feng, D.; Wu, Y.; Tan, X.; Chen, Q.; Yan, J.; Liu, M.; Ai, C.; Luo, Y.; Du, F.; Liu, S.; et al. Sensitive detection of melamine by an electrochemiluminescence sensor based on tris(bipyridine)ruthenium(II)-functionalized metal-organic frameworks. *Sens. Actuators B Chem.* **2018**, *265*, 378–386. [CrossRef]
28. Hong, D.; Jo, E.J.; Kim, K.; Song, M.B.; Kim, M.G. $Ru(bpy)_3^{2+}$-Loaded mesoporous silica nanoparticles as electrochemiluminescent probes of a lateral flow immunosensor for highly sensitive and quantitative detection of troponin I. *Small* **2020**, *16*, 2004535. [CrossRef]
29. Zhang, Q.; Liu, Y.; Nie, Y.; Ma, Q.; Zhao, B. Surface plasmon coupling electrochemiluminescence assay based on the use of AuNP@C_3N_4QD@mSiO_2 for the determination of the Shiga toxin-producing Escherichia coli (STEC) gene. *Microchim. Acta* **2019**, *186*, 656. [CrossRef]
30. Zhu, H.Y.; Ding, S.N. Dual-signal-amplified electrochemiluminescence biosensor for microRNA detection by coupling cyclic enzyme with CdTe QDs aggregate as luminophor. *Biosens. Bioelectron.* **2019**, *134*, 109–116. [CrossRef]
31. Fang, D.; Zhang, S.; Dai, H.; Lin, Y. An ultrasensitive ratiometric electrochemiluminescence immunosensor combining photothermal amplification for ovarian cancer marker detection. *Biosens. Bioelectron.* **2019**, *146*, 111768. [CrossRef] [PubMed]
32. Li, L.; Zhao, W.; Zhang, J.; Luo, L.; Liu, X.; Li, X.; You, T.; Zhao, C. Label-free Hg(II) electrochemiluminescence sensor based on silica nanoparticles doped with a self-enhanced $Ru(bpy)_3^{2+}$-carbon nitride quantum dot luminophore. *J. Colloid Interface Sci.* **2022**, *608*, 1151–1161. [CrossRef] [PubMed]
33. Xu, C.; Li, J.; Kitte, S.A.; Qi, G.; Li, H.; Jin, Y. Light scattering and luminophore enrichment-enhanced electrochemiluminescence by a 2D porous Ru@SiO_2 nanoparticle membrane and its application in ultrasensitive detection of prostate-specific antigen. *Anal. Chem.* **2021**, *93*, 11641–11647. [CrossRef] [PubMed]
34. Pan, D.; Chen, K.; Zhou, Q.; Zhao, J.; Xue, H.; Zhang, Y.; Shen, Y. Engineering of CdTe/SiO_2 nanocomposites: Enhanced signal amplification and biocompatibility for electrochemiluminescent immunoassay of alpha-fetoprotein. *Biosens. Bioelectron.* **2019**, *131*, 178–184. [CrossRef]
35. Li, L.; Chen, B.; Luo, L.; Liu, X.; Bi, X.; You, T. Sensitive and selective detection of Hg^{2+} in tap and canal water via self-enhanced ECL aptasensor based on NH_2–Ru@SiO_2-NGQDs. *Talanta* **2021**, *222*, 121579. [CrossRef] [PubMed]
36. Li, Z.; Zhang, J.; Chen, H.; Huang, X.; Huang, D.; Luo, F.; Wang, J.; Guo, L.; Qiu, B.; Lin, Z. Electrochemiluminescence biosensor for hyaluronidase based on the $Ru(bpy)_3^{2+}$ doped SiO_2 nanoparticles embedded in the hydrogel fabricated by hyaluronic acid and polyethylenimine. *ACS Appl. Bio Mater.* **2020**, *3*, 1158–1164. [CrossRef] [PubMed]
37. Liang, W.; Zhuo, Y.; Xiong, C.; Zheng, Y.; Chai, Y.; Yuan, R. A sensitive immunosensor via in situ enzymatically generating efficient quencher for electrochemiluminescence of iridium complexes doped SiO_2 nanoparticles. *Biosens. Bioelectron.* **2017**, *94*, 568–574. [CrossRef]
38. Mo, G.; He, X.; Zhou, C.; Ya, D.; Feng, J.; Yu, C.; Deng, B. A novel ECL sensor based on a boronate affinity molecular imprinting technique and functionalized SiO_2@CQDs/AuNPs/MPBA nanocomposites for sensitive determination of alpha-fetoprotein. *Biosens. Bioelectron.* **2019**, *126*, 558–564. [CrossRef]
39. Zhao, W.-R.; Xu, Y.H.; Kang, T.F.; Zhang, X.; Liu, H.; Ming, A.J.; Cheng, S.Y.; Wei, F. Sandwich magnetically imprinted immunosensor for electrochemiluminescence ultrasensing diethylstilbestrol based on enhanced luminescence of Ru@SiO_2 by CdTe@ZnS quantum dots. *Biosens. Bioelectron.* **2020**, *155*, 112102. [CrossRef]
40. Li, Y.; Liu, D.; Meng, S.; Zhang, J.; Li, L.; You, T. Regulation of $Ru(bpy)_3^{2+}$ electrochemiluminescence based on distance-dependent electron transfer of ferrocene for dual-signal readout detection of aflatoxin B1 with high sensitivity. *Anal. Chem.* **2022**, *94*, 1294–1301. [CrossRef]
41. Lee, E.J.; Seo, Y.; Park, H.; Kim, M.J.; Yoon, D.; Choung, J.W.; Kim, C.H.; Choi, J.; Lee, K.Y. Development of etched SiO_2@Pt@ZrO_2 core-shell catalyst for CO and C_3H_6 oxidation at low temperature. *Appl. Surf. Sci.* **2022**, *575*, 151582. [CrossRef]

42. Gu, Y.; Wu, Y.-n.; Li, L.; Chen, W.; Li, F.; Kitagawa, S. Controllable modular growth of hierarchical MOF-on-MOF architectures. *Angew. Chem. Int. Ed.* **2017**, *56*, 15658–15662. [CrossRef] [PubMed]
43. Long, J.; Gong, Y.; Lin, J. Metal–organic framework–derived Co_9S_8@CoS@CoO@C nanoparticles as efficient electro- and photocatalysts for the oxygen evolution reaction. *J. Mater. Chem. A* **2017**, *5*, 10495–10509. [CrossRef]
44. Fonseca, J.; Gong, T.; Jiao, L.; Jiang, H.-L. Metal–organic frameworks (MOFs) beyond crystallinity: Amorphous MOFs, MOF liquids and MOF glasses. *J. Mater. Chem. A* **2021**, *9*, 10562–10611. [CrossRef]
45. Miao, Y.B.; Ren, H.X.; Zhong, Q.; Song, F.X. Tailoring a luminescent metal−organic framework precise inclusion of Pt-Aptamer nanoparticle for noninvasive monitoring Parkinson's disease. *Chem. Eng. J.* **2022**, *441*, 136009. [CrossRef]
46. Wang, C.; Zhang, N.; Wei, D.; Feng, R.; Fan, D.; Hu, L.; Wei, Q.; Ju, H. Double electrochemiluminescence quenching effects of Fe_3O_4@PDA-Cu_XO towards self-enhanced $Ru(bpy)_3^{2+}$ functionalized MOFs with hollow structure and it application to procalcitonin immunosensing. *Biosens. Bioelectron.* **2019**, *142*, 111521. [CrossRef]
47. Yang, X.; Yu, Y.Q.; Peng, L.Z.; Lei, Y.M.; Chai, Y.Q.; Yuan, R.; Zhuo, Y. Strong electrochemiluminescence from MOF accelerator enriched quantum dots for enhanced sensing of trace cTnI. *Anal. Chem.* **2018**, *90*, 3995–4002. [CrossRef]
48. Dong, X.; Zhao, G.; Li, X.; Fang, J.; Miao, J.; Wei, Q.; Cao, W. Electrochemiluminescence immunosensor of "signal-off" for β-amyloid detection based on dual metal-organic frameworks. *Talanta* **2020**, *208*, 120376. [CrossRef]
49. Mo, G.; Qin, D.; Jiang, X.; Zheng, X.; Mo, W.; Deng, B. A sensitive electrochemiluminescence biosensor based on metal-organic framework and imprinted polymer for squamous cell carcinoma antigen detection. *Sens. Actuators B Chem.* **2020**, *310*, 127852. [CrossRef]
50. Dong, X.; Zhao, G.; Liu, L.; Li, X.; Wei, Q.; Cao, W. Ultrasensitive competitive method-based electrochemiluminescence immunosensor for diethylstilbestrol detection based on $Ru(bpy)_3^{2+}$ as luminophor encapsulated in metal–organic frameworks UiO-67. *Biosens. Bioelectron.* **2018**, *110*, 201–206. [CrossRef]
51. Nie, Y.; Tao, X.; Zhang, H.; Chai, Y.Q.; Yuan, R. Self-assembly of gold nanoclusters into a metal–organic framework with efficient electrochemiluminescence and their application for sensitive detection of rutin. *Anal. Chem.* **2021**, *93*, 3445–3451. [CrossRef] [PubMed]
52. Zhao, G.; Wang, Y.; Li, X.; Yue, Q.; Dong, X.; Du, B.; Cao, W.; Wei, Q. Dual-quenching electrochemiluminescence strategy based on three-dimensional metal–organic frameworks for ultrasensitive detection of amyloid-β. *Anal. Chem.* **2019**, *91*, 1989–1996. [CrossRef] [PubMed]
53. Dong, X.; Du, Y.; Zhao, G.; Cao, W.; Fan, D.; Kuang, X.; Wei, Q.; Ju, H. Dual-signal electrochemiluminescence immunosensor for Neuron-specific enolase detection based on "dual-potential" emitter $Ru(bpy)_3^{2+}$ functionalized zinc-based metal-organic frameworks. *Biosens. Bioelectron.* **2021**, *192*, 113505. [CrossRef]
54. Liu, H.; Liu, Z.; Yi, J.; Ma, D.; Xia, F.; Tian, D.; Zhou, C. A dual-signal electroluminescence aptasensor based on hollow Cu/Co-MOF-luminol and g-C_3N_4 for simultaneous detection of acetamiprid and malathion. *Sens. Actuators B Chem.* **2021**, *331*, 129412. [CrossRef]
55. Huang, W.; Hu, G.B.; Liang, W.B.; Wang, J.M.; Lu, M.L.; Yuan, R.; Xiao, D.R. Ruthenium(II) complex-grafted hollow hierarchical metal–organic frameworks with superior electrochemiluminescence performance for sensitive assay of thrombin. *Anal. Chem.* **2021**, *93*, 6239–6245. [CrossRef]
56. Wen, J.; Jiang, D.; Shan, X.; Wang, W.; Xu, F.; Shiigi, H.; Chen, Z. Ternary electrochemiluminescence biosensor based on black phosphorus quantum dots doped perylene derivative and metal organic frameworks as a coreaction accelerator for the detection of chloramphenicol. *Microchem. J.* **2022**, *172*, 106927. [CrossRef]
57. Xia, M.; Zhou, F.; Feng, X.; Sun, J.; Wang, L.; Li, N.; Wang, X.; Wang, G. A DNAzyme-based dual-stimuli responsive electrochemiluminescence resonance energy transfer platform for ultrasensitive anatoxin-a detection. *Anal. Chem.* **2021**, *93*, 11284–11290. [CrossRef]
58. Fang, J.; Li, J.; Feng, R.; Yang, L.; Zhao, L.; Zhang, N.; Zhao, G.; Yue, Q.; Wei, Q.; Cao, W. Dual-quenching electrochemiluminescence system based on novel acceptor CoOOH@Au NPs for early detection of procalcitonin. *Sens. Actuators B Chem.* **2021**, *332*, 129544. [CrossRef]
59. Huang, L.Y.; Hu, X.; Shan, H.-Y.; Yu, L.; Gu, Y.X.; Wang, A.J.; Shan, D.; Yuan, P.X.; Feng, J.J. High-performance electrochemiluminescence emitter of metal organic framework linked with porphyrin and its application for ultrasensitive detection of biomarker mucin-1. *Sens. Actuators B Chem.* **2021**, *344*, 130300. [CrossRef]
60. Hu, G.B.; Xiong, C.Y.; Liang, W.B.; Zeng, X.S.; Xu, H.L.; Yang, Y.; Yao, L.Y.; Yuan, R.; Xiao, D.R. Highly stable mesoporous luminescence-functionalized mof with excellent electrochemiluminescence property for ultrasensitive immunosensor construction. *ACS Appl. Mater. Interfaces* **2018**, *10*, 15913–15919. [CrossRef]
61. Wang, Y.; Zhao, G.; Chi, H.; Yang, S.; Niu, Q.; Wu, D.; Cao, W.; Li, T.; Ma, H.; Wei, Q. Self-luminescent lanthanide metal–organic frameworks as signal probes in electrochemiluminescence immunoassay. *J. Am. Chem. Soc.* **2021**, *143*, 504–512. [CrossRef] [PubMed]
62. Yan, M.; Ye, J.; Zhu, Q.; Zhu, L.; Huang, J.; Yang, X. Ultrasensitive immunosensor for cardiac troponin i detection based on the electrochemiluminescence of 2D Ru-MOF nanosheets. *Anal. Chem.* **2019**, *91*, 10156–10163. [CrossRef] [PubMed]
63. Zhao, L.; Wang, M.; Song, X.; Liu, X.; Ju, H.; Ai, H.; Wei, Q.; Wu, D. Annihilation luminescent Eu-MOF as a near-infrared electrochemiluminescence probe for trace detection of trenbolone. *Chem. Eng. J.* **2022**, *434*, 134691. [CrossRef]

64. Li, J.; Jia, H.; Ren, X.; Li, Y.; Liu, L.; Feng, R.; Ma, H.; Wei, Q. Dumbbell plate-shaped AIEgen-based luminescent MOF with high quantum yield as self-enhanced ECL tags: Mechanism insights and biosensing application. *Small* **2022**, *18*, 2106567. [CrossRef]
65. Huang, W.; Hu, G.B.; Yao, L.Y.; Yang, Y.; Liang, W.B.; Yuan, R.; Xiao, D.R. Matrix coordination-induced electrochemiluminescence enhancement of tetraphenylethylene-based hafnium metal–organic framework: An electrochemiluminescence chromophore for ultrasensitive electrochemiluminescence sensor construction. *Anal. Chem.* **2020**, *92*, 3380–3387. [CrossRef] [PubMed]
66. Yao, L.Y.; Yang, F.; Hu, G.B.; Yang, Y.; Huang, W.; Liang, W.B.; Yuan, R.; Xiao, D.R. Restriction of intramolecular motions (RIM) by metal-organic frameworks for electrochemiluminescence enhancement:2D Zr_{12}-adb nanoplate as a novel ECL tag for the construction of biosensing platform. *Biosens. Bioelectron.* **2020**, *155*, 112099. [CrossRef]
67. Zhou, L.; Yang, L.; Wang, C.; Jia, H.; Xue, J.; Wei, Q.; Ju, H. Copper doped terbium metal organic framework as emitter for sensitive electrochemiluminescence detection of CYFRA 21-1. *Talanta* **2022**, *238*, 123047. [CrossRef]
68. Wang, J.M.; Yao, L.Y.; Huang, W.; Yang, Y.; Liang, W.B.; Yuan, R.; Xiao, D.R. Overcoming aggregation-induced quenching by metal−organic framework for electrochemiluminescence (ECL) enhancement: Zn-PTC as a new ECL emitter for ultrasensitive MicroRNAs detection. *ACS Appl. Mater. Interfaces* **2021**, *13*, 44079–44085. [CrossRef]
69. Yao, L.Y.; Yang, F.; Liang, W.B.; Hu, G.B.; Yang, Y.; Huang, W.; Yuan, R.; Xiao, D.R. Ruthenium complex doped metal-organic nanoplate with high electrochemiluminescent intensity and stability for ultrasensitive assay of mucin 1. *Sens. Actuators B Chem.* **2019**, *292*, 105–110. [CrossRef]
70. Wang, C.; Li, Z.; Ju, H. Copper-doped terbium luminescent metal organic framework as an emitter and a co-reaction promoter for amplified electrochemiluminescence immunoassay. *Anal. Chem.* **2021**, *93*, 14878–14884. [CrossRef] [PubMed]
71. Ma, X.; Pang, C.; Li, S.; Li, J.; Wang, M.; Xiong, Y.; Su, L.; Luo, J.; Xu, Z.; Lin, L. Biomimetic synthesis of ultrafine mixed-valence metal–organic framework nanowires and their application in electrochemiluminescence sensing. *ACS Appl. Mater. Interfaces* **2021**, *13*, 41987–41996. [CrossRef]
72. Li, J.; Luo, M.; Jin, C.; Zhang, P.; Yang, H.; Cai, R.; Tan, W. Plasmon-enhanced electrochemiluminescence of PTP-decorated Eu MOF-Based Pt-tipped Au bimetallic nanorods for the lincomycin assay. *ACS Appl. Mater. Interfaces* **2022**, *14*, 383–389. [CrossRef] [PubMed]
73. Zhou, Y.; He, J.; Zhang, C.; Li, J.; Fu, X.; Mao, W.; Li, W.; Yu, C. Novel Ce(III)-metal organic framework with a luminescent property to fabricate an electrochemiluminescence immunosensor. *ACS Appl. Mater. Interfaces* **2020**, *12*, 338–346. [CrossRef] [PubMed]
74. Wang, X.; Xiao, S.; Yang, C.; Hu, C.; Wang, X.; Zhen, S.; Huang, C.; Li, Y. Zinc–metal organic frameworks: A coreactant-free electrochemiluminescence luminophore for ratiometric detection of miRNA-133a. *Anal. Chem.* **2021**, *93*, 14178–14186. [CrossRef] [PubMed]
75. Liu, Q.; Yang, Y.; Liu, X.P.; Wei, Y.P.; Mao, C.J.; Chen, J.S.; Niu, H.L.; Song, J.M.; Zhang, S.Y.; Jin, B.K.; et al. A facile in situ synthesis of MIL-101-CdSe nanocomposites for ultrasensitive electrochemiluminescence detection of carcinoembryonic antigen. *Sens. Actuators B Chem.* **2017**, *242*, 1073–1078. [CrossRef]
76. Sun, M.F.; Liu, J.L.; Zhou, Y.; Zhang, J.Q.; Chai, Y.Q.; Li, Z.H.; Yuan, R. High-efficient electrochemiluminescence of BCNO quantum dot-equipped boron active sites with unexpected catalysis for ultrasensitive detection of MicroRNA. *Anal. Chem.* **2020**, *92*, 14723–147299. [CrossRef] [PubMed]
77. Zhang, Q.; Liu, Y.; Nie, Y.; Liu, Y.; Ma, Q. Wavelength-dependent surface plasmon coupling electrochemiluminescence biosensor based on sulfur-doped carbon nitride quantum dots for K-RAS gene detection. *Anal. Chem.* **2019**, *91*, 13780–13786. [CrossRef]
78. Feng, D.; Wei, F.; Wu, Y.; Tan, X.; Li, F.; Lu, Y.; Fan, G.; Han, H. A novel signal amplified electrochemiluminescence biosensor based on MIL-53(Al)@CdS QDs and SiO_2@AuNPs for trichlorfon detection. *Analyst* **2021**, *146*, 1295–1302. [CrossRef]
79. Shan, X.; Pan, T.; Pan, Y.; Wang, W.; Chen, X.; Shan, X.; Chen, Z. Highly sensitive and selective detection of Pb(II) by $NH_2-SiO_2/Ru(bpy)_3^{2+}-UiO66$ based solid-state ECL sensor. *Electroanalysis* **2020**, *32*, 462–469. [CrossRef]
80. Cai, M.; Loague, Q.R.; Zhu, J.; Lin, S.; Usov, P.M.; Morris, A.J. Ruthenium(ii)-polypyridyl doped zirconium(iv) metal–organic frameworks for solid-state electrochemiluminescence. *Dalton Trans.* **2018**, *47*, 16807–16812. [CrossRef] [PubMed]
81. Zhao, L.; Song, X.; Ren, X.; Wang, H.; Fan, D.; Wu, D.; Wei, Q. Ultrasensitive near-infrared electrochemiluminescence biosensor derived from Eu-MOF with antenna effect and high efficiency catalysis of specific CoS_2 hollow triple shelled nanoboxes for procalcitonin. *Biosens. Bioelectron.* **2021**, *191*, 113409. [CrossRef]
82. Yang, Z.R.; Wang, M.M.; Wang, X.S.; Yin, X.B. Boric-acid-functional lanthanide metal–organic frameworks for selective ratiometric fluorescence detection of fluoride ions. *Anal. Chem.* **2017**, *89*, 1930–1936. [CrossRef] [PubMed]
83. Zhu, D.; Zhang, Y.; Bao, S.; Wang, N.; Yu, S.; Luo, R.; Ma, J.; Ju, H.; Lei, J. Dual intrareticular oxidation of mixed-ligand metal–organic frameworks for stepwise electrochemiluminescence. *J. Am. Chem. Soc.* **2021**, *143*, 3049–3053. [CrossRef]
84. Carrara, S.; Aliprandi, A.; Hogan, C.F.; De Cola, L. Aggregation-induced electrochemiluminescence of platinum(II) complexes. *J. Am. Chem. Soc.* **2017**, *139*, 14605–14610. [CrossRef] [PubMed]
85. Yang, Y.; Hu, G.B.; Liang, W.B.; Yao, L.Y.; Huang, W.; Zhang, Y.J.; Zhang, J.L.; Wang, J.M.; Yuan, R.; Xiao, D.R. An AIEgen-based 2D ultrathin metal–organic layer as an electrochemiluminescence platform for ultrasensitive biosensing of carcinoembryonic antigen. *Nanoscale* **2020**, *12*, 5932–5941. [CrossRef] [PubMed]
86. Li, J.; Jing, X.; Li, Q.; Li, S.; Gao, X.; Feng, X.; Wang, B. Bulk COFs and COF nanosheets for electrochemical energy storage and conversion. *Chem. Soc. Rev.* **2020**, *49*, 3565–3604. [CrossRef] [PubMed]

87. Zeng, W.J.; Wang, K.; Liang, W.B.; Chai, Y.Q.; Yuan, R.; Zhuo, Y. Covalent organic frameworks as micro-reactors: Confinement-enhanced electrochemiluminescence. *Chem. Sci.* **2020**, *11*, 5410–5414. [CrossRef] [PubMed]
88. Zhang, J.L.; Yao, L.Y.; Yang, Y.; Liang, W.B.; Yuan, R.; Xiao, D.R. Conductive covalent organic frameworks with conductivity and pre-reduction-enhanced electrochemiluminescence for ultrasensitive biosensor construction. *Anal. Chem.* **2022**, *94*, 3685–3692. [CrossRef] [PubMed]
89. Ravikumar, A.; Panneerselvam, P. A novel fluorescent sensing platform based on metal-polydopamine frameworks for the dual detection of kanamycin and oxytetracycline. *Analyst* **2019**, *144*, 2337–2344.
90. Ren, R.; Cai, G.; Yu, Z.; Zeng, Y.; Tang, D. Metal-polydopamine framework: An innovative signal-generation tag for colorimetric immunoassay. *Anal. Chem.* **2018**, *90*, 11099–11105. [CrossRef] [PubMed]
91. Ravikumar, A.; Panneerselvam, P.; Morad, N. Metal–polydopamine framework as an effective fluorescent quencher for highly sensitive detection of Hg(II) and Ag(I) ions through exonuclease III activity. *ACS Appl. Mater. Interfaces* **2018**, *10*, 20550–20558. [CrossRef] [PubMed]
92. Chen, A.; Zhao, M.; Zhuo, Y.; Chai, Y.; Yuan, R. Hollow porous polymeric nanospheres of a self-enhanced ruthenium complex with improved electrochemiluminescent efficiency for ultrasensitive aptasensor construction. *Anal. Chem.* **2017**, *89*, 9232–9238. [CrossRef] [PubMed]
93. Zhao, B.; Luo, Y.; Qu, X.; Hu, Q.; Zou, J.; He, Y.; Liu, Z.; Zhang, Y.; Bao, Y.; Wang, W.; et al. Graphite-like carbon nitride nanotube for electrochemiluminescence featuring high efficiency, high stability, and ultrasensitive ion detection capability. *J. Phys. Chem. Lett.* **2021**, *12*, 11191–11198. [CrossRef] [PubMed]
94. Malik, L.A.; Bashir, A.; Qureashi, A.; Pandith, A.H. Detection and removal of heavy metal ions: A review. *Environ. Chem. Lett.* **2019**, *17*, 1495–1521. [CrossRef]
95. Liao, H.; Jin, C.; Zhou, Y.; Chai, Y.; Yuan, R. Novel ABEI/dissolved O_2/Ag_3BiO_3 nanocrystals ECL ternary system with high luminous efficiency for ultrasensitive determination of MicroRNA. *Anal. Chem.* **2019**, *91*, 11447–11454. [CrossRef] [PubMed]
96. Gao, T.B.; Zhang, J.J.; Wen, J.; Yang, X.X.; Ma, H.B.; Cao, D.K.; Jiang, D. Single-molecule MicroRNA electrochemiluminescence detection using cyclometalated dinuclear Ir(III) complex with synergistic effect. *Anal. Chem.* **2020**, *92*, 1268–1275. [CrossRef]
97. Zhang, J.L.; Yang, Y.; Liang, W.B.; Yao, L.Y.; Yuan, R.; Xiao, D.R. Highly stable covalent organic framework nanosheets as a new generation of electrochemiluminescence emitters for ultrasensitive MicroRNA detection. *Anal. Chem.* **2021**, *93*, 3258–3265. [CrossRef] [PubMed]
98. Jiang, Y.; Li, R.; He, W.; Li, Q.; Yang, X.; Li, S.; Bai, W.; Li, Y. MicroRNA-21 electrochemiluminescence biosensor based on Co-MOF–N-(4-aminobutyl)-N-ethylisoluminol/$Ti_3C_2T_x$ composite and duplex-specific nuclease-assisted signal amplification. *Microchim. Acta* **2022**, *189*, 129. [CrossRef]
99. Jian, Y.; Wang, H.; Lan, F.; Liang, L.; Ren, N.; Liu, H.; Ge, S.; Yu, J. Electrochemiluminescence based detection of microRNA by applying an amplification strategy and Hg(II)-triggered disassembly of a metal organic frameworks functionalized with ruthenium(II)tris(bipyridine). *Microchim. Acta* **2018**, *185*, 133. [CrossRef] [PubMed]